Sensors & Transducers, Vol. 214, Issue 7, July 2017, pp. 21-27

www.sensorsportal.com

Sensors & Transducers

Published by IFSA Publishing, S. L., 2017
http://www.sensorsportal.com

LIBS Sensor for Sub-surface CO_2 Leak Detection in Carbon Sequestration

[1] Jinesh JAIN, [2] Dustin L. MCINTYRE, [2] Christian L. GOUEGUEL and [2] Chet R. BHATT

[1] National Energy Technology Laboratory, AECOM Technology Corporation, Pittsburgh, 15236, USA
[2] National Energy Technology Laboratory, U.S. Department of Energy, Pittsburgh, 15236, USA
[1] Tel.: 412-386-7470, fax: 412-386-4542
E-mail: Jinesh.Jain@netl.doe.gov

Received: 1 June 2017 /Accepted: 12 July 2017 /Published: 31 July 2017

Abstract: Monitoring carbon sequestration poses numerous challenges to the sensor community. For example, the subsurface environment is notoriously harsh, with large potential mechanical, thermal, and chemical stresses, making long-term stability and survival a challenge to any potential in situ monitoring method. Laser induced breakdown spectroscopy (LIBS) has been demonstrated as a promising technology for chemical monitoring of harsh environments and hard to reach places. LIBS has a real-time monitoring capability and can be used for the elemental and isotopic analysis of solid, liquid, and gas samples. The flexibility of the probe design and the use of fiber-optics has made LIBS particularly suited for remote measurements. The paper focuses on developing a LIBS instrument for downhole high-pressure, high-temperature brine experiments, where CO_2 leakage could result in changes in the trace mineral composition of an aquifer. The progress in fabricating a compact, robust, and simple LIBS sensor for widespread subsurface leak detection is presented.

Keywords: LIBS, C-Sequestration, Atomic spectroscopy, LIBS sensor, LIBS in drilling environments.

1. Introduction

Starting with the study of laser induced plasmas in the 1970s, Laser Induced Breakdown Spectroscopy (LIBS) has grown to become a productive measurement technique with a wide range of methods and applications being vigorously pursued around the globe [1]. LIBS uses one or more laser pulses to ablate and excite 1–1000 ng of sample mass into a plasma [2]. The light from the plasma contains wavelengths that are characteristic of the atomic emission from elements inside the plasma. To generate the high energies needed for plasma creation, lasers in LIBS instrumentation often rely on laser pulses shorter than a few tens of ns. In this fashion, a few mJ, or even tens of μJ energy, can create the high peak powers needed to overcome the dielectric breakdown of the material and produce the "spark" whereby the characteristic atomic emission light is generated.

Much of the recent growth in the field has come from the increasingly wide range of LIBS instruments developed in different laboratories and commercial entities [3]. In the commercial sector, these new instruments range from bench-top units that can be configured to operate in conjunction with laser ablation mass spectrometers to handheld devices configured for field use [4]. In like manner, there have also been several custom-designed instruments that

have taken LIBS into harsh environments, where typical approaches would be impossible. For example, the ChemCam installed on the Mars rover Curiosity uses LIBS to obtain detailed information about the elemental composition, geology, and geochemistry of the Martian surface [5]. The LIBS instrument the Chemi-Cam has also been used to probe the elemental composition of the deep ocean hydrothermal vents at 1 km depth [6]. Another instrument has been developed to analyze nuclear waste in underwater storage facilities [7]. It is difficult to imagine a conventional optical emission spectrometer that could have been used onsite in any of these applications. This paper describes development of a field deployable LIBS instrument for downhole measurement of CO_2 leak in carbon sequestration; a part of this study was presented in National Innovation Summit & Showcase, Washington, DC and published in TechConnect Briefs 2017 [8].

2. Background

By developing instruments for these unconventional environments, routes to tailored LIBS sensors for yet unexplored applications can emerge. One of such applications is the monitoring of geologic-sequestered CO_2 [9]. Geologic-carbon-sequestration (GCS) has the potential to store thousands of Gt (gigaton) of CO_2 in the United States alone [10]. In GCS, the CO_2 is prevented from entering the atmosphere, where it has been shown to be a major contributor to climate change. However, disposal of such large volumes in the sub-surface has potential to contaminate aquifers, so it will be important to verify that nearby underground sources of drinking water (USDW) are not be contaminated [11]. Several conventional methods for monitoring have been proposed, including pressure and temperature monitoring, seismic monitoring, and sample extraction for off-site analysis [12].

Given the array of potential failure of mechanisms for GCS, no single monitoring method can be regarded as sufficient to ensure containment alone. However, LIBS has the potential to play a central role in maximizing the confidence in detecting a CO_2 containment failure while minimizing the cost of implementing a monitoring system. One method of applying LIBS to the monitoring of CO_2 might be to analyze the total carbon content at or near the surface of the CO_2 disposal site. From an instrumentation perspective, this is the easiest way to monitor for leakage, and LIBS has been used in our laboratory to quantify changes in the carbon of air [13] and soil [14]. From a reliability perspective however, monitoring for CO_2 leakage at the surface is the most difficult. The various geologic formations, including those that comprise any caprock for storage, aquifers, and the vadose zone above the water table, serve to lens any potential CO_2 leakage and spread it out over a larger area [15, 16]. This constitutes a serious confounder for point detection, as the area of the leakage site at the surface is likely to dilute the CO_2 rise to that which would be below the background fluctuations.

As an alternative, LIBS can be used to analyze water from aquifers in or above the storage formation [17]. This is non-obvious, as direct measurement of carbon with LIBS, as has been done in air and soil is not feasible in the storage formation. First, the emission lines for carbon are located in the UV, where water is highly absorbing. Second, carbon analysis is difficult because the carbonate present in several aquifers can buffer pH and carbon content changes that might be induced by invasion of CO_2 into the aquifer, making direct measurement of carbon (or pH, for that matter) an imperfect method for detecting containment failure [18]. However, the buffering from resident mineral carbonate will also release cations such as calcium and potassium [19]. The cation release from these minerals is an unambiguous indicator of a pH change that might be the result of a containment failure. In this regard, the use of LIBS would be little different from a similar analysis using inductively coupled plasma optical emission spectroscopy (ICP-OES). In fact, the additional maturity and wide use of ICP-OES would make it an excellent tool for this kind of analysis.

What sets LIBS apart from ICP-OES and other CO_2 monitoring techniques is the potential to carry our measurements *in situ*. Although several kinds of sophisticated methods exist for extracting samples from monitoring wells for off-site analysis, the sample that is extracted nonetheless goes through several temperature and pressure changes prior to digestion and analysis in a benchtop spectrometer. These changes have the potential to induce precipitation of the very same cations being measured, thus introducing uncertainty into the measurement by means of the confounding precipitate. Having already demonstrated the capacity for use in harsh and extreme environments, LIBS has the potential to be deployed inside the monitoring well, monitoring the cationic composition of the aquifer at the temperature and pressure at depth and removing the potential confounders introduced by sample extraction.

3. LIBS in Downhole and Drilling Environments

The behavior of LIBS in aqueous conditions has been studied for the several decades now [20]. Most studies, however, have not focused on the kind of aqueous environment present in the subsurface. These can be highly saline and pressurized to tens to hundreds of atmospheres. These two variables constitute very strong matrix effects, causing variation in the pressure or salinity to change the LIBS spark characteristics of a given trace element.

There has been limited interest in the application of LIBS for *in situ* analysis in high-pressure aqueous environments such as in deep ocean hydrothermal vent fluids [21-25]. These studies have demonstrated LIBS for analysis of bulk solutions at pressures up to

300-400 bar, but several phenomena are not yet fully understood. Most of these studies are performed in a system pressurized with air, but not CO_2. The high-pressure CO_2 environment simulates conditions in CO_2 geologic storage applications and to provide a means of determining the feasibility for applying LIBS in subsurface GCS applications and conditions.

To evaluate the direct effect of elevated CO_2 on the LIBS signal, spectra at ambient conditions and at elevated CO_2 pressures were examined and compared. The plasma was formed in the presence of a pure carbon dioxide atmosphere at the given gas pressures (i.e., 10, 50, and 120 bar). The effect of pressure and water solubility on the LIBS signal was studied in an aqueous solution of 1000 mgL^{-1} calcium chloride ($CaCl_2 \cdot 2H_2O$), offering high signal-to-background ratio for the Ca I 422.67 nm emission line. The solution was prepared by dissolving $CaCl_2$ salt in ultrapure water.

Fig. 1 shows that the 422.67 nm Ca emission line intensity is dramatically reduced under high pressure CO_2 [26]. A CO_2 pressure of 10 bar produces a 37 % reduction and at 120 bar, the emission intensity drops by 70 %. These results are indicative of the direct effect of the gas pressure on Ca emission intensity.

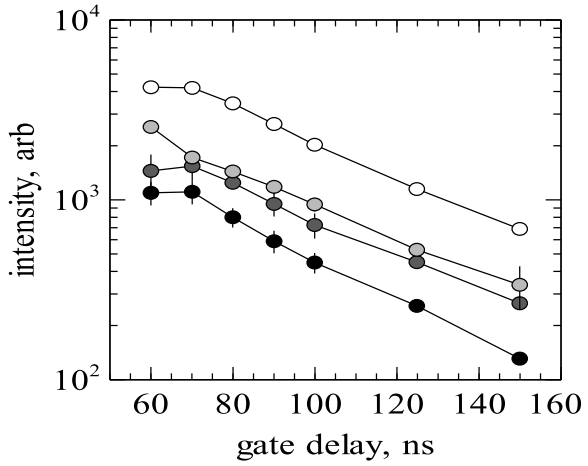

Fig. 1. Signal intensity of Ca I 422.67 nm emission lines as a function of gate delay for both ambient pressure (open circles) and at 10, 50, and 120 bar (light gray, dark gray, and filled circles, respectively) [26].

As is characteristic of the rapid cooling of plasma underwater, the Ca emission lines exhibit a short lifetime under different atmospheres and pressure conditions. The calcium neutral line exhibited emission lifetime in the range of 120 - 300 ns. A large difference between the intensity of the Ca lines obtained in ambient pressure and in the presence of CO_2 is observed for gate delays less than 100 ns. As the delay increases, the intensities decrease continuously with almost constant exponential decay as a function of pressure.

One factor that can contribute to the emission profile is the reaction between water and CO_2 to form carbonic acid ($H_2O_{(l)} + CO_{2(aq)} \leftrightarrow H_2CO_{3(aq)}$). Dissolved CO_2 in the form of carbonic acid may lose up to two protons through the acid equilibria to form bicarbonate and carbonate ions. These can react with cations (Ca^{2+}) in the aqueous solution to form a calcium carbonate solution and may lead to enhanced collisional excitation as a result.

The effect of elevated CO_2 pressure was also studied by measuring dissolution of $CaCO_3$ at different CO_2 pressures [27]. Pellets of pure $CaCO_3$ powder were immersed into a solution of $BaCl_2$. $BaCl_2$ served here as an internal standard. Spectra were recorded at ambient, 50, 150, 250, and 350 bar of CO_2 pressures and behavior of Ca and Ba lines with the increase in pressure was studied. Variation of FWHM of Ca I 422.67, Ca II 393.37, and Ba II 455.40 nm as a function of CO_2 pressure is presented in Fig. 2(a). Width of Ca I 422.67 and Ba II 455.40 nm lines increased with the pressure while that of the line Ca II 393.37 weakly depended on the pressure. Fig 2(b) shows the SBR for the Ca lines as a function of pressure. The SBRs slightly decreased as CO_2 is injected into the reactor and almost 30 % decrease was noticed when pressure reached to 350 bar. When intensity ratios of Ca lines with Ba line (Ca I/Ba II and Ca II/Ba II) were plotted as a function of CO_2 pressure, no significant effect of pressure was observed as shown in inset of Fig. 2 (b).

Likewise, the effects of high salinity on the LIBS emission spectra have received limited attention. For instance, Cremers, *et al.* [28] reported that the intensity ratio between the Ca II 393.37 nm and Ca I 422.67 nm lines decreases with the addition of sodium chloride (NaCl) to a 100 mgL^{-1} Ca-water solution. Michel, *et al.* [22] observed that the addition of 254 and 25400 mgL^{-1} NaCl to a solution of 1000 mgL^{-1} Ca (at 2.57×10^7 Pa) produced an increase in the emission intensity of the Ca I 422.67 nm line, while no significant increase was observed for the Ca II lines at 393.37 nm and 396.85 nm. Thornton, *et al.* [6] compared the spectra of Li and Ca obtained with and without 11,035 mgL^{-1} Na. They observed that Na enhanced the signal intensity of the Li (670 nm) and Ca (422.67 nm) lines. These studies are illustrative of the NaCl matrix effect on the LIBS signal of Ca.

Although the effect of cation-based matrix effect was studied, less so was the effect of anion based matrix effect. This is relevant to CO_2 storage because the chemical composition of groundwater is influenced by the minerals and gases reacting with the water in its relatively slow passage through the rocks and sediments of the Earth's crust. The geological formations at and around a storage site may include a wide range of minerals and the composition of these minerals may be affected when aqueous chemical equilibria are modified by the leaking CO_2. Water that circulates in limestone may contain bicarbonates/carbonates alkalinity. Chloride and sulfate are also present in groundwater. Because neither chloride nor sulfate takes part in typical biological or chemical reactions, they tend to concentrate in shallow groundwater over time.

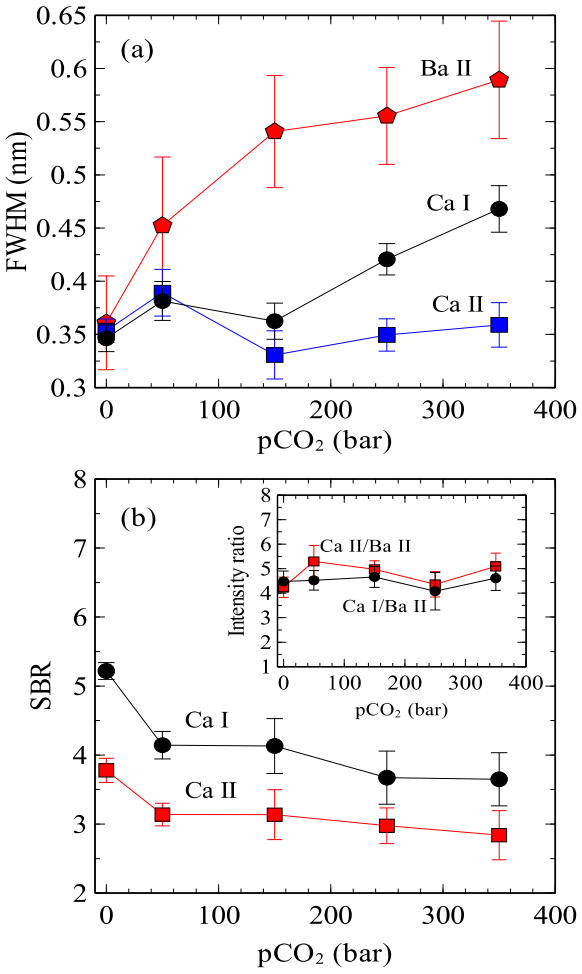

Fig. 2. (a) Full width at half maximum (FWHM) of Ca I 422.67 nm, Ca II 393.37 nm, and Ba II 455.40 nm lines, and (b) signal-to-background ratio (SBR) for Ca I 422.67 nm and Ca II 393.37 nm lines as a function of CO_2 pressure (pCO_2). The inset shows the comparison between the CaI/Ba II and Ca II/Ba II intensity ratios [27].

To examine the matrix effect of sodium salts of chloride, sulfate, and carbonate on the LIBS measurement of Li and K, we prepared solutions by mixing LiCl and KCl salts with NaCl, Na_2CO_3, and Na_2SO_4 [29]. Three sets of samples containing 10^3, 10^4, and 10^5 ppm of NaCl, Na_2CO_3, and Na_2SO_4 were prepared. By dividing the resulting LIBS signal by the expectation value from the calibration curve for that concentration, a normalized matrix effect can be estimated. This normalized matrix effect for Li^+ and K^+ is plotted in Fig. 3 for the three mentioned salts. As evidence of matrix effect, a clear dependence of sample matrix can be seen on the Li I and K I emission line intensities. For NaCl, an increase in the intensity of the emission lines is observed with the addition of 0.1 – 1 % NaCl. For Na_2CO_3, there is a reduction in the emission line intensities across all concentrations. However, for Na_2SO_4, there is a little change compared to the control solution, even at 10 % salt concentration. Generally, the normalized matrix effect shows a slight decrease in the signal as a function of trace metal concentration.

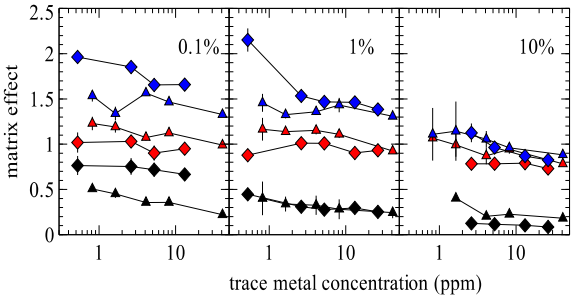

Fig. 3. The effect of 0.1, 1, and 10 % solutions of NaCl (blue), Na_2SO_4 (red), and Na_2CO_3 (black) on the calibration curves of Li^+ (▲) and K^+ (◆) is shown. The *y*-axis displays the measured intensity divided by the value given by the calibration curve for that concentration [26].

A comparison of matrix effects indicates that in the presence of dissolved sodium compounds the emission line intensities vary in the following order: NaCl > Na_2SO_4 > Na_2CO_3. For instance, when compared to the pure solution, the intensity of Li emission line obtained in LiCl + 1000 ppm NaCl and LiCl + 1000 ppm Na_2SO_4 samples ([Li+] = 1.6 ppm) increases by 2- and 1.5-fold, whereas the line intensity decreases by half using LiCl + 1000 ppm Na_2CO_3 sample. This behavior seems to be related to the difference of thermal properties between aqueous NaCl, Na_2SO_4 and Na_2CO_3, such as boiling point (NaCl, 1690 K; Na_2SO_4, 1700 K; Na_2CO_3, 1870 K) and thermal conductivity (NaCl, 6.5 $W \cdot m^{-1} K^{-1}$; Na_2SO_4, 1.0 $W \cdot m^{-1} K^{-1}$; Na_2CO_3, 0.6 $W \cdot m^{-1} K^{-1}$ at 300 K). Fig. 3 also shows that underwater LIBS signal is detectable in high salinity water (i.e. for a sodium salt concentration up to 10^5 ppm), thereby demonstrating the feasibility of using LIBS for saline groundwater monitoring.

4. LIBS Sensor Instrumentation

In order to apply LIBS in downhole and drilling environments, modification in LIBS configuration may be required accordingly. Often, for example, the spectrometer is placed near or adjacent to the pulsed laser. Many successful variations on this arrangement have been reported in the literature in well controlled laboratory settings. However, in a downhole application, this arrangement would require that much of the most expensive and sensitive components be placed in an inaccessible and dangerous environment. For some optical applications, the beam path can be fiber-coupled, which allows all the equipment to remain at the surface, as is done in distributed acoustic sensing. Unfortunately, the peak laser pulse energies required to generate LIBS sparks in aqueous environments are much higher than the thresholds of conventional optical fibers. By separating the measurement head from the spectrometer, we are allowed to keep the more expensive equipment at the surface, reducing the engineering burden and cost of deployment. The measurement head also needs to be

fabricated in such a way it is (1) small, (2) robust and (3) low cost. This would allow the least expensive components to be placed in the most dangerous environment, again minimizing the engineering burden and cost of deployment.

Another important consideration is the type and configuration of pulsed laser that would be used. Many of the laboratory studies carried out on aqueous LIBS have amply demonstrated the benefits of the double-pulse LIBS (DP-LIBS) [25]. In this configuration, the first laser pulse is used to initiate the formation of a bubble or cavity. The second pulse is the one from which the LIBS light is collected. This has been shown to produce a higher quality signal than the conventional single-pulse LIBS. As desirable as this may be, there is substantial cost and complexity to the use of a DP-LIBS approach for downhole applications, most of which would hinge around the difficulty of timing the second pulse. To properly and precisely trigger the second laser pulse at the appointed time, an active Q-switch laser would be necessary, which would add substantial difficulty to the measurement. Accommodating the equipment necessary for active Q-switch lasers – Pockels cell, waveplate, output coupler, high reflector, polarizer, gain medium, and pump source – in the well bore is possible, but not without substantial cost and complexity. Furthermore, as useful as this may be, we have demonstrated successful use of single-pulse LIBS in synthetic brines at temperature.

Instead of the common active Q-switch laser, we have proposed the use of a passive Q-switch laser that is fiber coupled to an end-pump and spectrometer, as depicted in Fig. 4 [26]. The passive Q-switch allows the laser to be driven only by a pump laser at the surface that is fiber-coupled to the end-pumped laser rod downhole. Once the laser fires and spark is generated, the light from the spark can be directed around the laser rod and back into the optical fiber. By use of a pulse detector, the LIBS spectrometer can be triggered to capture the spectrum at a specific gate delay. Once the spectrum is recorded, it can be transmitted in digital format over to a computer that handles the power, data storage, processing, and control of the instrument. This allows all the electronic circuitry to remain at the surface, where the risks (and detector array temperature) can be more easily controlled, while allowing the LIBS measurement to be taken at depth.

Our first prototype is shown below in Fig. 5. It consists of a passive Q-switch laser rod that is affixed inside of a housing. The housing is constructed from components purchased from Thorlabs and modified with light machining and customization.

The housing contains a fiber coupler, pump laser focusing lens, and pulsed laser focusing lens. The entire assembly is only 6.2 cm in length, 1.3 cm in width, and 32 g in weight. At economies of scale, the device cost would be a small fraction of the rest of the equipment necessary to carry out a LIBS measurement. This initial design can be modified to accommodate the requirements of a downhole LIBS system, but it is also suitable for other applications with tight mass and volume requirements.

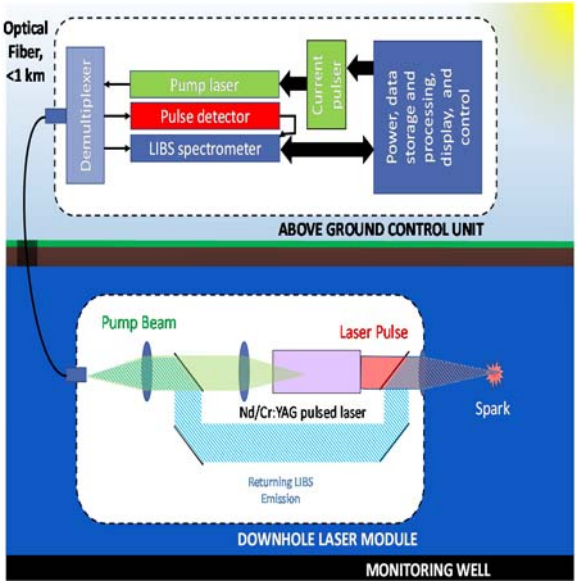

Fig. 4. A schematic for operation of a downhole LIBS monitoring system with a control unit above ground. The control unit has the pump laser, spectrometer, and timing circuitry to operate the pulsed laser and measure the LIBS signal. The downhole laser module is equipped with a separate beam path that allows the LIBS light to be coupled back into the optical fiber connected to the control unit.

Fig. 5. On the top, a model of the passive Q-switch laser and, on the bottom, the finished prototype [26].

5. Conclusions

The work presented here outlines how LIBS can be adapted to the unique challenges of downhole environments. Besides using in carbon sequestration, LIBS sensor has other multiple potential applications.

It can be used for in-situ measurements of elemental, molecular, and physical measurements of any matter irrespective of its physical state and environmental condition [30-32]. It could be a robust alternative technique for oil and gas industries to make downhole measurements of liquids, gases, and rocks including Marcellus Shale [33]. The gas capacity can be correlated with the organic and inorganic content of the shale. Furthermore, all the elements present in any source, including minerals and rare earth elements (REEs) in hydrothermal vents at elevated pressure can be detected with LIBS sensor [34-36]. As the technologies develop, LIBS may well be acquire the ability to deploy additional capabilities beyond elemental concentration monitoring in harsh environments, such as Raman spectroscopy [37] and Laser Ablation Molecular Isotopic Mass Spectrometry (LAMIS) [38], which would allow for a wider range of measurements to be carried out by a robust, remote LIBS probe. The continued development of LIBS for these applications has the potential to migrate LIBS from the laboratory to the field site and crucial measurements and services along the way.

References

[1]. F. Anabitarte, A. Cobo, J. M. Lopez-Higuera, Laser-induced breakdown spectroscopy: fundamentals, applications, and challenges, *International Scholarly Research Notices,* Vol. 2012, 2012.

[2]. D. A. Cremers, L. J. Radziemski, Introduction, in Handbook of Laser-Induced Breakdown Spectroscopy, ed. *John Wiley & Sons Ltd*, 2013, pp. 1-27.

[3]. D. W. Hahn, N. Omenetto, Laser-induced breakdown spectroscopy (LIBS), part II: Review of instrumental and methodological approaches to material analysis and applications to different fields, *Appl. Spectrosc.*, Vol. 66, No. 4, 2012, pp. 347–419.

[4]. D. Day, B. Connors, M. Jennings, J. Egan, K. Derman, P. Soucy, *et al.*, A full featured handheld LIBS analyzer with early results for defense and security, in *SPIE Sensing Technology+ Applications*, 2015, pp. 948206-1–948206-7.

[5]. S. Maurice, R. Wiens, M. Saccoccio, B. Barraclough, O. Gasnault, O. Forni, *et al.*, The ChemCam instrument suite on the Mars Science Laboratory (MSL) rover: science objectives and mast unit description, *Space Science Reviews,* Vol. 170, Issue 1-4, 2012, pp. 95-166.

[6]. B. Thornton, T. Takahashi, T. Sato, T. Sakka, A. Tamura, A. Matsumoto, *et al.*, Development of a deep-sea laser-induced breakdown spectrometer for in situ multi-element chemical analysis, *Deep Sea Research Part I: Oceanographic Research Papers,* Vol. 95, 2015, pp. 20-36.

[7]. A. Whitehouse, J. Young, I. Botheroyd, S. Lawson, C. Evans, J. Wright, Remote material analysis of nuclear power station steam generator tubes by laser-induced breakdown spectroscopy, *Spectrochimica Acta Part B: Atomic Spectroscopy,* Vol. 56, Issue 6, 2001, pp. 821-830.

[8]. J. Jain, D. McIntyre, C. Goueguel, Harsh environment low cost LIBS sensor for sub-surface CO2 leak detection in carbon sequestration, *Materials for Energy, Efficiency and Sustainability: TechConnect Briefs 2017,* in *Proceedings of the National Innovation Summit & Showcase*, Washington, DC, 2017.

[9]. C. M. White, B. R. Strazisar, E. J. Granite, J. S. Hoffman, H. W. Pennline, Separation and capture of CO2 from large stationary sources and sequestration in geological formations—coalbeds and deep saline aquifers, *Journal of the Air & Waste Management Association,* Vol. 53, No. 6, 2003, pp. 645-715.

[10]. R. Wright, F. Mourits, L. B. Rodríguez, M. D. Serrano, The First North American Carbon Storage Atlas, *Energy Procedia,* Vol. 37, 2013, pp. 5280-5289.

[11]. C. M. Oldenburg, S. L. Bryant, J.-P. Nicot, Certification framework based on effective trapping for geologic carbon sequestration, *International Journal of Greenhouse Gas Control,* Vol. 3, No. 4, 2009, pp. 444-457.

[12]. S. I. Plasynski, J. T. Litynski, H. G. McIlvried, D. M. Vikara, R. D. Srivastava, The critical role of monitoring, verification, and accounting for geologic carbon dioxide storage projects, *Environmental Geosciences,* Vol. 18, No. 1, 2011, pp. 19-34.

[13]. V. Dikshit, F.-Y. Yueh, J. P. Singh, D. L. McIntyre, J. C. Jain, N. Melikechi, Laser induced breakdown spectroscopy: A potential tool for atmospheric carbon dioxide measurement, *Spectrochimica Acta Part B: Atomic Spectroscopy,* Vol. 68, 2012, pp. 65-70.

[14]. K. K. Ayyalasomayajula, F. Yu-Yueh, J. P. Singh, D. L. McIntyre, J. Jain, Application of laser-induced breakdown spectroscopy for total carbon quantification in soil samples, *Applied Optics,* Vol. 51, Issue 7, 2012, pp. B149-B154.

[15]. C. M. Oldenburg, A. J. Unger, On leakage and seepage from geologic carbon sequestration sites, *Vadose Zone Journal,* Vol. 2, No. 3, 2003, pp. 287-296.

[16]. C. M. Oldenburg, A. J. Unger, Coupled vadose zone and atmospheric surface-layer transport of carbon dioxide from geologic carbon sequestration sites, *Vadose Zone Journal,* Vol. 3, Issue 3, 2004, pp. 848-857.

[17]. J. Jain, D. Mcintyre, K. Ayyalasomayajula, V. Dikshit, C. Goueguel, F. Yu-Yueh, *et al.*, Application of laser-induced breakdown spectroscopy in carbon sequestration research and development, *Pramana,* Vol. 83, Issue 2, 2014, pp. 179-188.

[18]. N. Assayag, J. Matter, M. Ader, D. Goldberg, P. Agrinier, Water–rock interactions during a CO2 injection field-test: implications on host rock dissolution and alteration effects, *Chemical Geology,* Vol. 265, Issue 1-2, 2009, pp. 227-235.

[19]. J. M. Matter, T. Takahashi, D. Goldberg, Experimental evaluation of in situ CO_2-water-rock reactions during CO_2 injection in basaltic rocks: Implications for geological CO_2 sequestration, *Geochemistry, Geophysics, Geosystems,* Vol. 8, Issue 2, 2007.

[20]. R. Knopp, F. Scherbaum, J. Kim, Laser induced breakdown spectroscopy (LIBS) as an analytical tool for the detection of metal ions in aqueous solutions, *Fresenius' Journal of Analytical Chemistry,* Vol. 355, Issue 1, 1996, pp. 16-20.

[21]. M. Lawrence-Snyder, J. Scaffidi, S. M. Angel, A. P. Michel, A. D. Chave, Laser-induced breakdown spectroscopy of high-pressure bulk aqueous solutions, *Applied Spectroscopy,* Vol. 60, Issue 7, 2006, pp. 786-790.

[22]. A. P. Michel, M. Lawrence-Snyder, S. M. Angel, A. D. Chave, Laser-induced breakdown spectroscopy of bulk aqueous solutions at oceanic pressures:

evaluation of key measurement parameters, *Applied Optics,* Vol. 46, Issue 13, 2007, pp. 2507-2515.
[23]. V. N. Rai, F.-Y. Yueh, J. P. Singh, Study of laser-induced breakdown emission from liquid under double-pulse excitation, *Applied Optics,* Vol. 42, Issue 12, 2003, pp. 2094-2101.
[24]. A. P. Michel, A. D. Chave, Double pulse laser-induced breakdown spectroscopy of bulk aqueous solutions at oceanic pressures: interrelationship of gate delay, pulse energies, interpulse delay, and pressure, *Applied Optics,* Vol. 47, Issue 31, 2008, pp. G131-G143.
[25]. M. Lawrence-Snyder, J. Scaffidi, S. M. Angel, A. P. Michel, A. D. Chave, Sequential-pulse laser-induced breakdown spectroscopy of high-pressure bulk aqueous solutions, *Applied Spectroscopy,* Vol. 61, Issue 2, 2007, pp. 171-176.
[26]. C. G. Carson, C. Goueguel, J. Jain, D. McIntyre, Development of laser-induced breakdown spectroscopy sensor to assess groundwater quality impacts resulting from geologic carbon sequestration, in *SPIE Defense+ Security*, *Proc. SPIE 9467, Micro- and Nanotechnology Sensors, Systems, and Applications VII,* 2015, pp. 94671K-1–94671K-15.
[27]. C. L. Goueguel, J. C. Jain, D. L. McIntyre, C. G. Carson, H. M. Edenborn, In situ measurements of calcium carbonate dissolution under rising CO_2 pressure using underwater laser-induced breakdown spectroscopy, *Journal of Analytical Atomic Spectrometry,* Vol. 31, No. 7, 2016, pp. 1374-1380.
[28]. D. A. Cremers, L. J. Radziemski, T. R. Loree, Spectrochemical analysis of liquids using the laser spark, *Applied Spectroscopy,* Vol. 38, Issue 5, 1984, pp. 721-729.
[29]. C. Goueguel, D. L. McIntyre, J. Jain, A. K. Karamalidis, C. Carson, Matrix effect of sodium compounds on the determination of metal ions in aqueous solutions by underwater laser-induced breakdown spectroscopy, *Applied Optics,* Vol. 54, Issue 19, 2015, pp. 6071-6079.
[30]. P. Moreschini, K. Zacny, G. Paulsen, Laser induced breakdown spectroscopy for downhole analysis of lunar regolith, in *Proceedings of the 42nd Lunar and Planetary Science Conference*, 2011.
[31]. R. S. Harmon, F. C. DeLucia, C. E. McManus, N. J. McMillan, T. F. Jenkins, M. E. Walsh, *et al.*, Laser-induced breakdown spectroscopy - An emerging chemical sensor technology for real-time field-portable, geochemical, mineralogical, and environmental applications, *Applied Geochemistry,* Vol. 21, Issue 5, May 2006, pp. 730-747.
[32]. C. Bohling, K. Hohmann, D. Scheel, C. Bauer, W. Schippers, J. Burgmeier, *et al.*, All-fiber-coupled laser-induced breakdown spectroscopy sensor for hazardous materials analysis, *Spectrochimica Acta Part B: Atomic Spectroscopy,* Vol. 62, Issue 12, 2007, pp. 1519-1527.
[33]. H. K. Sanghapi, J. Jain, A. Bol'shakov, C. Lopano, D. McIntyre, R. Russo, Determination of Elemental Composition of Shale Rocks by Laser Induced Breakdown Spectroscopy (LIBS), *Spectrochimica Acta Part B: Atomic Spectroscopy,* Vol. 122, 2016, pp. 9-14.
[34]. C. R. Bhatt, F. Y. Yueh, J. P. Singh, Univariate and multivariate analyses of rare earth elements by laser-induced breakdown spectroscopy, *Applied Optics,* Vol. 56, Issue 8, 2017, pp. 2280-2287.
[35] D. Alamelu, A. Sarkar, S. Aggarwal, Laser-induced breakdown spectroscopy for simultaneous determination of Sm, Eu and Gd in aqueous solution, *Talanta,* Vol. 77, Issue 1, 2008, pp. 256-261.
[36]. V. Lazic, S. Jovicevic, Laser induced breakdown spectroscopy inside liquids: Processes and analytical aspects, *Spectrochimica Acta Part B: Atomic Spectroscopy,* Vol. 101, 1 Nov. 2014, pp. 288-311.
[37]. G. B. Courreges-Lacoste, B. Ahlers, F. R. Pérez, Combined Raman spectrometer/laser-induced breakdown spectrometer for the next ESA mission to Mars, *Spectrochimica Acta Part A: Molecular and Biomolecular Spectroscopy*, Vol. 68, Issue 4, 2007, pp. 1023-1028.
[38]. A. A. Bol'shakov, X. Mao, J. Jain, D. L. McIntyre, R. E. Russo, Laser ablation molecular isotopic spectrometry of carbon isotopes, *Spectrochimica Acta Part B: Atomic Spectroscopy*, Vol. 113, 2015, pp. 106-112.